Accepted Article

Title: Visible-Light Photoswitchable Benzimidazole Azo-Arenes as beta-Arrestin2-Biased Selective Cannabinoid 2 Receptor Agonists

Authors: Sophie A. M. Steinmueller, Julia Fender, Marie H. Deventer, Anna Tutov, Kristina Lorenz, Christophe P. Stove, James Hislop, and Michael Decker

WILEY•VCH

RESEARCH ARTICLE

Visible-Light Photoswitchable Benzimidazole Azo-Arenes as β-Arrestin2-Biased Selective Cannabinoid 2 Receptor Agonists

Sophie A. M. Steinmüller, Julia Fender, Marie H. Deventer, Anna Tutov, Kristina Lorenz, Christophe P. Stove, James N. Hislop, and Michael Decker*

[*]   S. A. M. Steinmüller, A. Tutov, Prof. Dr. Michael Decker
        Pharmazeutische und Medizinische Chemie
        Institut für Pharmazie und Lebensmittelchemie
        Julius-Maximilians-Universität Würzburg
        Am Hubland, 97074 Würzburg (Germany)
        E-mail: michael.decker@uni-wuerzburg.de

        M. H. Deventer, Prof. Dr. C. Stove
        Laboratory of Toxicology, Department of Bioanalysis
        Faculty of Pharmaceutical Sciences
        Ghent University
        Ottergemsesteenweg 460, 9000 Ghent (Belgium)

        J. Fender, Prof. Dr. Kristina Lorenz
        Institut für Pharmakologie und Toxikologie,
        Julius-Maximilians-Universität Würzburg
        Versbacher Str. 9, 97078 Würzburg (Germany)

        Prof. Dr. Kristina Lorenz
        Leibniz-Institut für Analytische Wissenschaften - ISAS-e.V.
        Bunsen-Kirchhoff-Straße 11, 44139 Dortmund, Germany (Germany)

        Dr. J. N. Hislop
        School of Medicine, Medical Sciences and Nutrition
        Institute of Medical Sciences
        University of Aberdeen
        Foresterhill, Aberdeen AB25 2ZD (United Kingdom)

        Supporting information for this article is given via a link at the end of the document.

Abstract: The cannabinoid 2 receptor (CB$_2$R) has high therapeutic potential for multiple pathogenic processes, such as neuroinflammation. Pathway-selective ligands are needed to overcome the lack of clinical success and to elucidate correlations between pathways and their respective therapeutic effects. Herein, we report the design and synthesis of a photoswitchable scaffold based on the privileged structure of benzimidazole and its application as a functionally selective CB$_2$R "efficacy-switch". Benzimidazole azo-arenes offer huge potential for the broad extension of photopharmacology to a wide range of optically addressable biological targets. We used this scaffold to develop compound **10d**, a "*trans*-on" agonist, which serves as a molecular probe to study the β-arrestin2 (βarr2) pathway at CB$_2$R. βArr2 bias was observed in CB$_2$R internalization and βarr2 recruitment, while no activation occurred when looking at Gα$_{16}$ or mini-Gα$_i$. Overall, compound **10d** is the first light-dependent functionally selective agonist to investigate the complex mechanisms of CB$_2$R-βarr2 dependent endocytosis.

Introduction

The endocannabinoid system (ECS) consists of G protein-coupled receptors (GPCRs), mainly cannabinoid receptor subtypes 1 and 2 (CB$_1$R and CB$_2$R), their endogenous ligands and several enzymes involved in synthesis or degradation of endocannabinoids.[1] CB$_1$R is highly abundant in the central nervous system (CNS), but is also distributed in peripheral tissues, such as the heart, liver or gastrointestinal tract, while CB$_2$R is predominantly expressed in peripheral tissues with immune functions, including spleen, tonsils, leukocytes and macrophages.[2] CB$_2$R expression was found to be induced in both the periphery and the CNS in response to immune system activation and inflammation, as well as in microglial cells surrounding amyloid-β plaques in Alzheimer's disease (AD) patients. Microglia, as the resident macrophages of the CNS, do not express CB$_2$Rs in their unstimulated form.[2a, 3] A reduction of microglia-mediated neurotoxicity due to the release of pro-inflammatory cytokines was achieved by application of selective CB$_2$R agonists.[4] Moreover, CB$_2$R agonism was found to cause microglial migration, which promotes enhanced phagocytosis of amyloid-β plaques.[4-5]

The ECS has been associated with therapeutic potential for multiple diseases. Especially CB$_2$R was found to play an important role in the pathogenesis of inflammatory or neuropathic pain, neurodegenerative diseases such as AD, as well as in autoimmune diseases and diverse cancer types.[6] Currently more than 30% of all drugs approved by the US Food and Drug Administration (FDA) target GPCRs.[7] However, targeting CB$_1$R and CB$_2$R has not yet led to the desired therapeutic success. The complexity of the ECS and its involvement in numerous

RESEARCH ARTICLE

physiological processes and functions such as memory, appetite, immune functions, pain modulation and neuroprotection – to name just a few – makes it difficult to get the desired therapeutic effects without implication of severe adverse effects.[8] The most prominent example of failed CB therapeutics is probably still the CB_1R-selective inverse agonist rimonabant, which had been approved by the FDA in 2006 for treatment of obesity and was then again withdrawn from the market in 2008 due to psychiatric adverse effects.[8c, 9] The therapeutic interest has since shifted further towards CB_2R. Selectivity of cannabinoid ligands towards CB_2R over CB_1R is desirable to avoid the well-known psychoactive effects of (-)-*trans*-Δ9-tetrahydrocanabinol resulting from CB_1R agonism.[10] CB_2R-selective agonists are non-psychoactive and may lead to fewer side effects due to restricted expression of CB_2R in the CNS.[6b, 6c]

There is still too little known about the pharmacological aspects of CB_2R signaling in both healthy and pathogenic processes. CB_2R ligands show high structural variability and exhibit pronouncedly heterogenous signaling profiles. Many of such ligands, especially endocannabinoids, display pathway-preferential signaling. This phenomenon is referred to as "biased signaling" and can cause a "functionally selective" response.[11] Endocannabinoids have shown bias for G protein activation while having none to low efficacy regarding βarr recruitment.[12] This large discrepancy in signaling might serve to explain or contribute to the failure (so far) of many CB_2R ligands in clinical trials and highlights the importance of functionally selective CB_2R ligands.[12b, 13] While the G protein pathway has been well-studied, there is much less known about the function of βarr at CB_2R.[14] Recently, βarr2 recruitment to CB_2R has been associated with tolerance development whilst showing analgesic effects in an osteoarthritis model.[15] Overall, the pharmacological impact of βarr recruitment at CB_2R is not yet completely understood and further steps must be taken to evaluate the role of βarr activation with regard to therapeutic potential or adverse effects.

Photoswitchable compounds offer the potential to serve as valuable tools to study pharmacological processes at receptor level and have proven useful in the field of medicinal chemistry and molecular biology. Photopharmacological compounds allow optical control over their targeted receptor or enzyme by application of external light sources. Such photoswitchable ligands isomerize upon irradiation with certain wavelengths in a way that they function as a reversible "switch", ideally between an inactive and an active isomer, which allows precise temporal control over receptor activation.[16] To date, great progress has been made using such photoswitchable compounds to successfully investigate pharmacological processes at GPCRs, including class A dopaminergic receptors,[17] serotonin receptors,[18] adrenergic receptors,[19] muscarinic receptors[20] as well as CBRs,[21] and several class B and C GPCRs.[22] In order to fully understand specific signaling pathways and their biological response, pathway-selective photoswitchable tool compounds would be particularly useful. To the authors' knowledge, only one biased photoswitchable ligand has been reported in literature so far. Broichhagen *et al.* developed "LirAzo", a photoswitchable incretin mimetic with isomer-biased signaling. While *cis*-LirAzo promotes cyclic adenosine monophosphate production significantly more than its *trans*-photoisomer, *trans*-LirAzo preferentially induced Ca^{2+}-signaling.[22b] Enabling time-controlled optical activation of a particular pathway of CB_2R with a functionally selective ligand is a major step towards identification

of the therapeutic potential or the thread of adverse effects associated with this specific signaling pathway. A βarr-biased photoswitchable ligand could shed light onto the previously discussed potential adverse effects associated with the βarr pathway. The understandings gained by using such a tool compound could finally facilitate the successful development of advanced therapeutic candidates.

Previous work from our group used a benzimidazole structure developed by AstraZeneca to obtain a CB_2R-selective "*cis*-on"-affinity photoswitchable ligand via the azo-extension approach.[21a] For the present work, we continued to use this scaffold for designing biased photoswitchable ligands as "efficacy switches" for CB_2R by introducing a photoswitchable moiety in the 2-position of the benzimidazole. Many GPCR ligands,[23] enzyme inhibitors,[24] antiviral[25] or anticancer[26] compounds are built from a benzimidazole scaffold which is known for its high pharmacological significance due to its broad range of biological activities resulting from different substitution patterns at the core structure.[27] To date, several benzimidazole derivatives are available as approved drugs.[27b, 28] In the case of CB_2R, benzimidazoles were used to design potent selective agonists and inverse agonists.[23c, 29] Making this privileged structure photoswitchable directly at its core will most probably contribute towards obtaining optical control over diverse targets. Furthermore, heteroarene photoswitches have recently gained importance due to their high tunability.[30] While 2-benzimidazole azo-arenes have been synthesized before,[31] their photoswitchable behavior has not yet been investigated. Several photoswitchable CBR-probes have recently been described in literature. Our group very recently developed "photo-rimonabant", which is a rimonabant-derived photoswitchable CB_1R antagonist with 15-fold higher affinity in its *cis*-photoisomer.[21d] Major contributions towards obtaining optical control over CB_2R were made by the Carreira group in 2021 and by Tao and coworkers in the same year.[21b, 21c] Therewith, R. C. Sarott *et al.* developed photoswitchable derivatives of HU308 enabling optical control over Ca^{2+} release in AtT-22(CB_2) cells, with both a *cis*- and *trans*-active compound.[21b] Furthermore, Hu *et al.* used the CB_2R antagonist AM10257 to obtain a photoswitchable CB_2R antagonist with a 44-fold higher IC_{50} value for the *cis*-compound following an atypical azobenzene remodeling approach.[21c]

Our photoswitchable 2-benzimidazole azo-arenes show a distinguished signaling profile at CB_2R with βarr2 bias. Compound **10d** was shown to act as "efficacy switch" for activating the βarr2 pathway while not activating G protein pathways. In addition, this newly characterized photoswitchable scaffold has superior photophysical properties compared to regular azobenzene and enables visible-light optical control. Our synthesized compounds were photocharacterized and analyzed in different biological assays validating the pharmacological differences between the respective photoisomers.

Results and Discussion

Many heterogenous but promising scaffolds of CB_2R ligands can be found in literature, of which several were used for the design of photoswitchable ligands. Based on the results previously obtained in our group, a ligand with benzimidazole core structure was pursued. The potent, selective CB_2R agonist **1** (**Figure 1**) has

RESEARCH ARTICLE

been used in our group as a template to obtain a photochromic CB$_2$R "affinity switch" by incorporating an azobenzene.[21a] Structure-affinity relationships (SARs) established by AstraZeneca highlighted the benzene ring substitution pattern as an important, sensitive feature by showing that small changes of the substitution pattern can influence efficacy *in vitro*. By simply introducing a constraint for the *p*-ethoxy group, efficacy was inverted and **2** was shown to be a potent, selective CB$_2$R inverse agonist.[23c, 29]
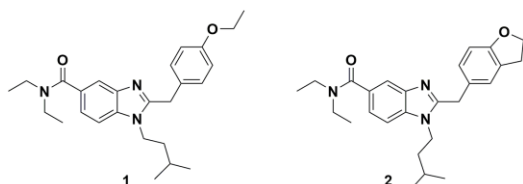
Figure 1. Benzimidazole-based lead structures for *h*CB$_2$R agonists.

Recognizing the potential to influence efficacy in this susceptible position, the scaffold was sought out for the design of an "efficacy switch". To obtain light-dependent spatial control over this sensitive position, an azo-bond was introduced into the scaffold to connect the benzimidazole with the benzene ring, thereby forming benzimidazole azo-arenes (see **Figure 2**).
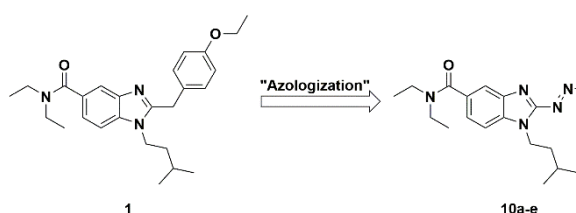
Figure 2. Non-classical azologization approach to obtain 2-benzimidazole azo-arenes.

We designed and synthesized five derivatives of benzimidazole azo-arenes (**10a-e**) derived from compound **1** (see **Scheme 1**). By replacing the methylene unit with an azo bond, the molecular structure as well as electronic properties are altered. The benzylic tail at 2-position of the benzimidazole is prolonged and might not be in the same spatial orientation as in parent compound **1**. Due to these structural changes, it was unclear whether *para*-substitution at the benzene would still result in the same spatial orientation compared to parent compound **1**. Therefore, the ethoxy ether was at first attached both in *meta*-position (**10a**) as well as in *para*-position (**10b**). Then, after observing a bigger *cis*/*trans*-difference regarding CB$_2$R affinity for *para*-substitution, which most probably occurs due to spatially affecting this sensitive position, substitution of further derivatives was chosen accordingly. Next, a methoxy group was introduced as a smaller substituent (**10c**) to compensate possible prolongation of the structure due to the introduction of a photoswitchable moiety. Instead of the phenolic ethyl ether, a methoxymethyl-phenyl substituent was attached (**10d**) as a constitutional isomer with a different position of the oxygen in the alkyl chain. This was done to investigate whether introduction of the azo bond requires a different oxygen-position for benzimidazole azo-arenes and if the oxygen position or electronic effects are important for interaction

with the receptor and thereby influence affinity/efficacy with potentially even a more pronounced *cis*/*trans*-difference. Furthermore, isopropyl substitution (**10e**) was chosen to investigate whether interaction is based primarily on steric effects and to potentially highlight the importance of the oxygen, which was always kept during assessment of SARs for parent compounds **1** and **2**. Target compounds were tested regarding their affinity in radioligand binding assays and were further evaluated for their ability to activate G protein (Gα_{16} and Gα_i) as well as βarr2 pathways.
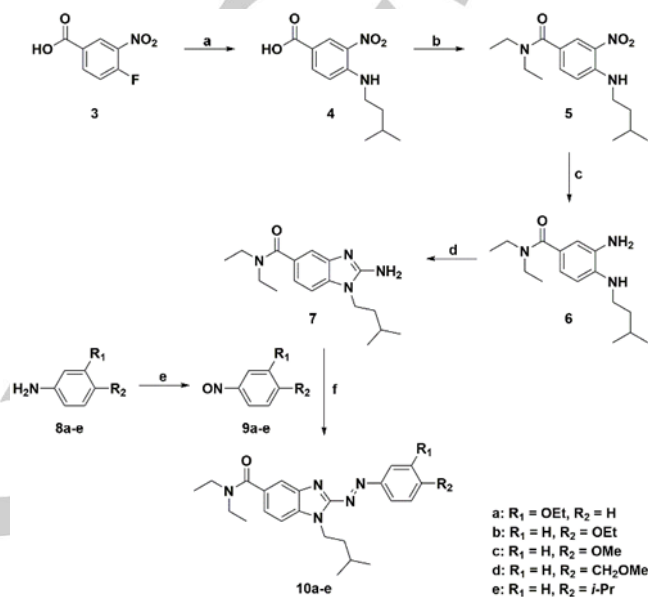
Scheme 1. Synthesis of 2-benzimidazole azo-arenes. Reagents and conditions: (a) 3-methylbutylamine, MeOH, rt, 2 h; (b) i. HBTU, *N,N*-dimethylformamide (DMF), rt, 30 min; ii. NHEt$_2$, NEt$_3$, DMF, rt, 8 h; (c) H$_2$, Pd/C, MeOH, rt, 21 h; (d) BrCN, rt, overnight; (e) Oxone®, dichloromethane/water, rt, 2-16 h; (f) toluene/NaOH (40%, aq.) 1:1 (2 mL/mmol), 80°C, 2-4 h.

Benzimidazole azo-arenes were synthesized from a 2-aminobenzimidazole derivative and the respective nitroso compounds in a modified Baeyer-Mills reaction (c.f. **Scheme 1**). The 2-aminobenzimidazole precursor (**7**) was synthesized from commercially available 4-fluoro-3-nitrobenzoic acid (**3**). Nucleophilic aromatic substitution with isopentyl amine gave quantitative yields of compound **4**. The amide (**5**) was then formed using diethyl amine and HBTU. Reduction of the nitro group was done using hydrogen and Pd/C to give aniline **6** in quantitative yields. Synthesis of compound **6** has previously been described by our group using different reduction conditions,[32] but yields could be improved using a more common palladium reduction. The 2-benzimidazoleamine (**7**) was at first formed using the nonhazardous 1,3-bis(tert-butoxycarbonyl)-2-methyl-2-thio-pseudourea as previously described in literature.[25] As this approach only yielded low amounts of the Boc-aminobenzimidazole as well as the Boc-deprotected compound (**7**), ring closure was then achieved with cyanogen bromide in high yields (> 90%). The respective nitroso compounds (**9a-e**) were obtained by partial oxidation of the respective anilines with Oxone®. Finally, a modified Baeyer-Mills reaction was carried out under basic conditions using a 1:1 mixture of 40% NaOH and toluene, a versatile method described by Fuchter and coworkers

RESEARCH ARTICLE

for synthesizing arylazopyrazoles that demonstrably works for a broader range of azo-heteroarenes.[33]

To characterize this novel photoswitchable scaffold regarding its photophysical properties, compounds **10a-e** were analyzed by UV/vis spectroscopy using both a 30 μM solution in DMSO and in Tris-buffer (pH = 7.4) to confirm reversible photoisomerization and to preclude possible photo-fatigue (**SI Figure S1-S5**). Light of different wavelengths between 365 nm and 590 nm was used to determine the ideal switching wavelengths. All 2-benzimidazole azo-arenes showed the highest photoconversion to the *cis*-configuration with visible light (λ = 400 nm), thereby showing "red-shifted" behavior compared to regular azobenzenes which have the highest *cis*-conversion after irradiation with UV light (λ = 365 nm).[34] Photoisomerization back to the *trans*-photoisomers of benzimidazole azo-arenes was achieved with either green (λ = 530 nm, **10a** and **10e**) or orange light (λ = 590 nm, **10b-d**), enabled by the long wavelength absorption tail of the respective *cis*-photoisomer.
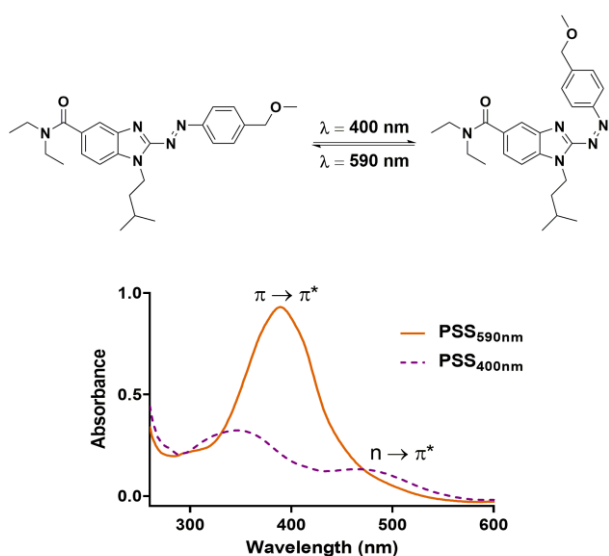

Figure 3. Representative photoisomerization of **10d** (30 μM in aqueous Tris-buffer, pH = 7.4) and its UV absorbance spectrum after irradiation with purple light (λ = 400 nm, purple dashed line) and orange light (λ = 590nm, solid orange line), respectively.

The absorption spectrum of lead compound **10d** is shown in **Figure 3**. For regular azobenzenes, the absorption spectra consist of a large absorption band around 325 nm corresponding to $\pi \rightarrow \pi^*$ transitions and a smaller tailing absorption band at 430 nm corresponding to $n \rightarrow \pi^*$ transitions. This was found to be consistent in arylazoimidazoles with slightly shifted absorption maxima at 361-375 nm ($\pi \rightarrow \pi^*$) and at around 450 nm ($n \rightarrow \pi^*$).[35] In the case of 2-benzimidazole azo-arenes, these absorption maxima are even further red-shifted to 383-402 nm ($\pi \rightarrow \pi^*$) and approximately 500 nm ($n \rightarrow \pi^*$), depending on the substitution at the benzene ring. Alternate irradiation with purple (λ = 400 nm) and orange (λ = 590 nm) or green (λ = 530 nm) light showed reversible photoconversion between the respective *cis*- and *trans*-enriched states of all compounds. Photochromic behavior was stable for many switching cycles and thus, no photo-fatigue occurred (for compound **10d**, see **Figure 4**).
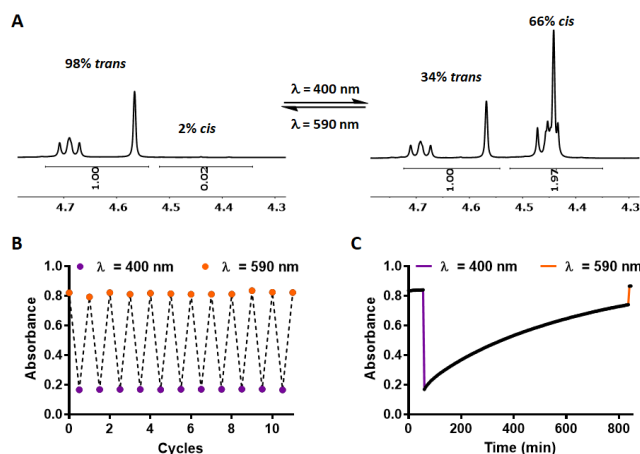

Figure 4. Photophysical characterization of compound **10d**. (A) Determination of *cis/trans* ratios via peak shifting analyzed in CD₃OD in ¹H NMR-spectroscopy after irradiation with orange light (λ = 590nm, left) and purple light (λ = 400 nm, right). The ¹H signals of aryl-C<u>H</u>₂-O-CH₃ and N-C<u>H</u>₂ (isopentyl) were shifted upfield upon photoisomerization and were used for calculation of the PSD. (B) Switching cycles of compound **10d** (30 μM in aqueous Tris-buffer, pH=7.4) without any noticeable photofatigue. (C) Thermal stability measurement of 30 μM *cis*-**10d** after irradiation with 400 nm in Tris-buffer/10% DMSO (pH = 7.4, ambient temperature); monitored for 13 h and switched back to its *trans*-photoisomer with 590 nm.

Thermal stability of 2-benzimidazole azo-arenes was monitored in DMSO and aqueous Tris-buffer (pH=7.4, containing 10 % DMSO) and differed with substituents and their position at the benzene ring (**Table 1**). Electron-withdrawing substituents in *para*-position have previously been shown to decrease thermal *cis→trans* relaxation time in azobenzenes.[36] For benzimidazole azo-arenes, introduction of the *p*-ethoxy ether (**10b**) resulted in a shorter half-life than for the *meta*-derivative (**10a**). This correlation was consistent in DMSO and aqueous buffer solution, with half-lives being considerably shorter in buffer. Shortening of the substituent to a *p*-methoxy ether (**10c**) further decreased the half-life in DMSO. This is in accordance with the observation that thermal relaxation of substituted azobenzenes is solvent dependent and half-lives were found to be shorter, especially in aqueous physiological solution due to hydrogen bonding.[34] In contrast, for 2-benzimidazole azo-arene **10d**, thermal relaxation was found to take longer in aqueous buffer solution compared to DMSO. Overall, our benzimidazole azo-arenes show excellent thermal half-lives in DMSO and in buffer, also in comparison to other photoswitchable azo-heteroarene scaffolds.[37]

Photostationary distribution (PSD), *i.e.* the ratio of respective *cis*- and *trans*-photoisomers obtained after irradiation with a certain wavelength, was determined using ¹H NMR spectroscopy and confirmed using HPLC-MS (see **Table 1**). The respective *trans*-photoisomers were obtained in high, and in some cases almost quantitative, yields after irradiation with orange (λ = 590 nm) or green (λ = 530 nm) light. However, a fraction of the respective compound remains in its *trans*-form even after irradiation with purple light (λ = 400 nm). Such PSDs are however not uncommon when looking at visible-light switchable azoheteroarenes.[38] This incomplete switching might lead to an underestimation of the effects caused by the *cis*-photoisomer of the respective compound when applied in a biological setting. However, biological systems in principle follow a nonlinear nature and distinct biological effects can be caused despite having poorly defined *cis/trans* ratios.[34]

4

RESEARCH ARTICLE

Table 1. Photoconversion of 2-benzimidazole azo-arenes as determined by HPLC in MeOH and ^{1}H NMR spectroscopy, and thermal stability of *cis*-photoisomers in DMSO and Tris-buffer/10% DMSO (pH = 7.4) at ambient temperature.

Compound	$\lambda_{cis \to trans}$, % *trans*-isomer[a]	$\lambda_{trans \to cis}$, % *cis*-isomer[a]	$t_{1/2}$ [min] in DMSO[b]	$t_{1/2}$ [min] in buffer[b]
10a	83	70	345	251
10b	99	60	126	1.8
10c	96	68	81.8	4.6
10d	98	67	245	346
10e	89	78	200	170

[a] Highest obtainable amount of *cis*- or *trans*-photoisomers after irradiation with the respective optimal wavelength for isomerization. PSDs were determined after illumination with the respective wavelength by ^{1}H NMR spectroscopy or by HPLC-MS (in MeOH) at the respective isosbestic point. Ratios were not dependent on the method or concentration. [b] 400 nm light was used to trigger excitation to the *cis*-photoisomer; absorption of the respective 30 µM solution was measured for at least 8 h (data provided in supporting information).

As all synthesized compounds were found to be photoswitchable upon investigation of their photophysical properties, it was decided to assess whether these configurational changes also affect affinity at CB_2 or selectivity over CB_1 receptors. Affinities of the respective *cis*- and *trans*-enriched states were analyzed using radioligand binding studies (see **Table 2**, **SI Figure S6**). As this assay is carried out at room temperature and can be performed under light exclusion, isomerization between the different photoisomers due to light exposure is effectively avoided. On the other hand, continuous irradiation of the plates during the incubation time is also possible and required for compounds with short half-lives. Thus, false-negative or false-positive results due to isomerization between the photoisomers during the 3 h incubation time can be avoided. The respective *cis*-photoisomers of the test compounds required irradiation with purple light (λ = 400 nm) either continuously or at least every 20 minutes to avoid back-isomerization and to make sure that the *cis*/*trans*-ratios upon measurement were the same as previously determined. It was confirmed beforehand that irradiation did not influence binding affinity for reference compound **1** for which we obtained a K_i of 27 nM. All tested compounds showed affinity towards CB_2R in the micromolar range (**Table 2**). Structural changes for obtaining a photoswitchable molecule (*i.e.*, introducing an azo-bond in potentially sensitive positions) can lead to a certain affinity loss,[39] which is however tolerated if the compound achieves the overall aim for reversible photocontrol of a certain receptor.[18a] For *meta*-substitution at the benzene ring of the benzimidazole azo-arene scaffold (**10a**), no difference in the binding affinities was observed for the two photoisomers. The *cis*-photoisomers of the *para*-substituted benzimidazole azo-arenes exhibited higher affinities towards CB_2R ("*cis*-on"-affinity), with **10d** having the highest difference between the photoisomers regarding this key pharmacological parameter. The *cis*-enriched state of **10d**, obtained by irradiation with purple light, has a 6.5-fold higher affinity than in its thermodynamically more stable *trans*-state (**Figure 5A**). Keeping in mind that the described *cis*-enriched state of **10d** still contains about 34% of the *trans*-compound, the actual difference in affinity will even be higher.

Table 2. Affinity values at *r*CB_1R and *h*CB_2R determined by radioligand binding studies.

Compound/ Photoisomer		*r*CB_1 K_i [µM] (-pIC_{50} ± SEM) or [^{3}H]CP55940 displ. at 1 µM	CB_2 *trans*/ *cis* ratio	*h*CB_2 K_i [µM] (-pIC_{50} ± SEM)
1		< 10%	-	0.027 (7.56 ± 0.056)
Rimonabant		0.056 (7.16 ± 0.056)	-	-
CP55940		0.0088 (8.02 ± 0.054)		0.013 (7.86 ± 0.071)
10a	*cis*	< 10%	1.3	9.1 (5.02 ± 0.060)
	trans	< 10%		12 (4.89 ± 0.087)
10b	*cis*	< 10%	3.0	5.0 (5.28 ± 0.066)
	trans	< 10%		15 (4.80 ± 0.065)
10c	*cis*	< 10%	1.9	4.3 (5.35 ± 0.055)
	trans	< 10%		8.3 (5.06 ± 0.067)
10d	*cis*	10%	6.5	1.3 (5.86 ± 0.033)
	trans	< 10%		8.4 (5.05 ± 0.064)
10e	*cis*	< 10%	2.7	1.6 (5.79 ± 0.060)
	trans	< 10%		4.3 (5.35 ± 0.058)

To analyze G protein dependent efficacy, the 2-benzimidazole azo-arenes were evaluated in a *h*CB_2R $G\alpha_{16}$-coupled fluorescent calcium mobilization assay. Stably transfected Chinese hamster ovary (CHO) K1 cells overexpressing *h*CB_2R were used to monitor intracellular calcium response with Fluo-4AM. Compounds **10a-e** were tested in both photoisomers. As the compounds were shown to reliably photoisomerize in buffer, compound dilutions in buffer were irradiated with the respective wavelength directly prior to the experiment. Reference compound **1** and CP55940 (EC_{50} = 21.4 nM) were used as controls for CB_2R agonism (**SI Figure S7**). Despite this assay having a lower sensitivity for substances in the micromolar range, agonist response can be monitored quite easily. Reference compound **1** behaved as an agonist at CB_2R with nanomolar efficacy (EC_{50} = 54.0 nM). To our surprise, none of the synthesized 2-benzimidazole azo-arene derivatives showed efficacy in Ca^{2+} mobilization in either photoisomeric state at concentrations from 10 nM up to 30 µM (**SI Figure S7**). Only for *cis*-**10b** a weak agonistic response was detectable with a maximal activation (E_{max}) of 15%, while compounds **10c** and **10e** seem to behave as inverse agonists.

To further analyze the nature of compounds **10a-e** regarding their ability to activate a non-chimeric G protein pathway, a NanoBiT® luciferase assay, monitoring mini-$G\alpha_i$ recruitment to *h*CB_2R, was evaluated. Additionally, βarr2 recruitment was analyzed using a similar NanoBiT® assay. Based on three independent experiments, compounds **10a**, **10b** and **10d** (in non-irradiated state) did not show signs of mini-$G\alpha_i$ recruitment at concentrations up to 1 µM, although a (limited) potential to recruit βarr2 was found for **10a**, **10b** and **10d**. For all three compounds, higher concentrations (100 µM, 10 µM) resulted in a substantial decrease in luminescent signal in both assays (for CB_2 mini-$G\alpha_i$,

RESEARCH ARTICLE

see **SI Figure S8**). To evaluate whether this phenomenon was hCB$_2$R-dependent, high concentrations of the compounds were screened in an orthogonal assay using µ opioid (MOR)- βarr2 NanoBiT®. Similar "inactivation" profiles at MOR were noticed, signifying that the pronounced decrease in luminescence is not CB$_2$R specific (data not shown). A plausible hypothesis for this phenomenon lies within the properties of the tested compounds. Stock solutions containing the highest concentrations of **10a**, **10b** and **10d** are brightly orange colored. Considering the absorption spectra (**SI Figure S1–S5**), higher compound concentrations likely result in the absorption of a portion of the luminescence emitted by the nanoluciferase enzyme (emission wavelength 460 nm).[40] This intrinsic limitation of the nanoluciferase enzyme hampers the analysis of higher concentrations of these compounds.

Comparing mini-Gα_i and βarr2, no bias factor could be calculated due to the aforementioned assay limitations and a lack of activity in the mini-Gα_i pathway. However, data presented in **Figure S9** (Supporting Information) does indicate that there may be a preferential recruitment of βarr2, as lower concentrations of **10a** and **10b** can still result in recruitment of βarr2, whereas the same concentrations were inactive in the mini-Gα_i recruitment assay.

As **10a**, **10b** and **10d** did show some βarr2 recruitment potential, both photoisomeric states were tested in various concentrations using the hCB$_2$-βarr2 assay. Stock solutions were irradiated with the respective wavelengths prior to the experiment, and for both photoisomers, CP55940 served as the reference standard. All three compounds were found to be weakly active in the hCB$_2$-βarr2 bioassay, with negligible differences in activity between the *cis*- and *trans*-photoisomers. Overall, **10b** had the highest activity in the hCB$_2$-βarr2 recruitment assay, with a maximal activation of 23% (*cis*) and 18% (*trans*), relative to CP55940, at the highest test concentration (500 nM), followed by **10a** with a relative efficacy of 15% for both photoisomers. Compound **10d** was found to have the lowest activity, with an efficacy of <5% for the *cis*-photoisomer and 6% for the *trans*-photoisomer, relative to the E$_{max}$ of CP55940, set at 100% (**SI Figure S10**). It is expected that analyzing higher concentrations (1 µM and higher) would result in a higher efficacy for all three compounds. However, due to the encountered intrinsic limitations, high concentrations were not included and sigmoidal dose-response curves therefore not fully recorded. Similarly, differences in activity comparing the photoisomers, as well as the potency of the compounds (EC$_{50}$), could not be assessed accurately, as the plateau of maximal activation was not reached and hence, no statements regarding potential *cis/trans*-differences could be made.

As some βarr2 recruitment was observed for the compounds, activation of CB$_2$R was then investigated using confocal microscopy to monitor receptor internalization which is functionally linked to the βarr2 pathway, as knockdown of βarr2 expression was shown to inhibit CB$_2$R internalization[41]. While βarr recruitment has been observed for some GPCRs lacking functional G proteins, it did not result in G protein independent signaling and was proposed to either control surface abundance of GPCRs via the endocytic pathway or to allow for signaling from inside the cell.[42] Compound **10d**, which has the highest *cis/trans*-difference regarding CB$_2$R affinity, was investigated using confocal microscopy with human embryonic kidney (HEK) 293 cells stably expressing FLAG-epitope-tagged hCB$_2$R (F-hCB$_2$R) and detected with AlexaFluor™-568 conjugated antiFLAG-M1

antibody. The data indicates that the compound is able to induce CB$_2$R internalization, with *trans*-**10d** being more efficient than its *cis*-photoisomer (see **Figure S14**, SI), which is surprising given the higher CB$_2$R-affinity of *cis*-**10d**. However, due to the nature of the constitutive receptor trafficking (see untreated sample in **Figure S14**, SI), quantification was difficult.

To circumvent these limitations and to further evaluate whether preferred recruitment of βarr2 may indeed translate to βarr2 bias, the compounds were analyzed in a flow cytometry based CB$_2$R internalization assay, which had previously been useful for accurate quantification of internalization.[43] Efficacy of the 2-benzimidazole azo-arenes was evaluated regarding their effect on βarr2-mediated endocytosis of F-hCB$_2$R, stably expressed in HEK293 cells, detected by fluorescently conjugated antiFlag-M1 antibody, monitored by flow cytometry.[43b] Agonist response was expressed as percentage of CP55940-caused internalization. Dilutions were done in DMSO and irradiated with the respective wavelength before addition to the wells. For analyzing the *cis*-photoisomer, irradiation of the 12-well plates was carried out additionally three times during the incubation time of 45 min at 37°C to keep the compounds in their respective *cis*-enriched state. Parent compound **1** proved to be a full agonist in endocytosis with nanomolar efficacy (EC$_{50}$ (CB$_2$R) = 2.7 nM), and efficacy was not impaired by irradiation. All compounds were initially evaluated for their effect on CB$_2$R endocytosis at 1 µM concentration (**SI Figure S11**). The most potent compounds **10a**, **10b** and **10d** were chosen for establishing dose-response curves of the respective photoisomers. For the *meta*-substituted 2-benzimidazole azo-arene **10a**, no *cis/trans*-difference could be observed regarding efficacy in CB$_2$R endocytosis, which is consistent with radioligand binding results. Both photoisomers were partial agonists (E$_{max}$ = 43-46%), with a similar EC$_{50}$ in the sub-micromolar range (EC$_{50}$ (CB$_2$R) = 300 nM, **SI Figure S12B**). Upon moving the ethoxy-function from *meta*- to *para*-position (**10b**), the *cis*-photoisomer becomes a more potent partial agonist (EC$_{50}$ (CB$_2$R) = 25.1 nM; E$_{max}$ = 41%) than its corresponding *trans*-photoisomer (EC$_{50}$ (CB$_2$R) = 49.8 nM; E$_{max}$ = 32%; **SI Figure S12C**). This indicates that *para*-substitution, as was the case for parent compound **1**, is still favorable for 2-benzimidazole azo-arenes at CB$_2$R. Compound **10d** behaved as a partial agonist at CB$_2$R in its *trans*-photoisomer, with a sub-micromolar EC$_{50}$ = 139 nM (E$_{max}$ = 51%). Despite the *cis*-photoisomer of **10d** having a 6.5-fold higher affinity towards CB$_2$R, the measured efficacy reached an E$_{max}$ of only 22%, with a similar EC$_{50}$ = 153 nM compared to its *trans*-photoisomer (**Figure 5B**). A plausible explanation for this phenomenon could be the observed incomplete photoisomerization to the *cis*-photoisomer, which still includes 34% of the *trans*-photoisomer in the *cis*-enriched state. This difference in E$_{max}$ is consistent with confocal microscopy data and confirms that *trans*-**10d** is a more efficient agonist when looking at internalization. We hypothesize that *p*-ethoxy substitution (**10b**) of the benzimidazole azo-arene scaffold still has the right length and spatial orientation for addressing CB$_2$R (weak "*cis*-on" efficacy). However, while some affinity is lost when changing the oxygen position in its constitutional isomer **10d**, on the other hand this led to improved photophysical and photopharmacological properties which are more suitable in the investigated setting. The most promising compound **10d** thereby shows very interesting pharmacological properties, as it is a "*cis*-on"-affinity switch but a "*trans*-on"-efficacy switch (**Figure 5**). Thus, binding affinity of compound **10d** at CB$_2$R is higher in the inactive form (PSS$_{400nm}$)

RESEARCH ARTICLE

and decreases upon irradiation with orange light (PSS$_{590nm}$), which appears to be accompanied by unlocking activation of the βarr2 pathway. As this assay is not limited by interference of compound absorption with the readout for the fluorescently labeled antibody (Excitation/Emission 650/665 nm), full dose-response curves could be measured. As this assay seems to be more sensitive than the radioligand binding assay, all compounds were again tested against CB$_1$R to study selectivity. No agonist response could be observed at 1 µM concentration regarding the amount of internalized CB$_1$R for neither of the respective photoisomers, thereby elucidating excellent CB$_2$R-selectivity of the synthesized 2-benzimidazole azo-arenes.

Figure 6. Detection of ERK phosphorylation by Western blot analysis. Activation of ERK1/2 by CB$_2$R ligands was examined by evaluating ERK1/2 phosphorylation (pERK1/2) at the TEY motif in response to CP55940 (10 µM) or the *cis-* and *trans*-photoisomers of compound **10d** (0.1 µM or 1.0 µM) for 8 minutes. Total ERK1/2 was used as loading control.

βArr binding has long been associated with receptor desensitization only but was found to also modulate G protein-dependent downstream signaling like extracellular signal-regulated kinase (ERK) activation.[11a, 14, 42] To investigate the effects of both reference compound CP55940 and target compound **10d**, in both *cis-* and *trans*-photoisomers, we conducted Western blot analyses to evaluate the phosphorylation of ERK1/2 at the TEY motif.[45] The phosphorylation of the TEY motif is essential for the enzymatic activity of these kinases. Following an 8-minute stimulation, we observed a concentration-dependent increase in ERK1/2 activation for both photoisomers of compound **10d**. Additionally, we found that *trans*-**10d** induced a greater degree of ERK1/2 phosphorylation than its *cis*-photoisomer, as shown in **Figure 6**. This further confirms that the "*trans*-on"-efficacy behavior of compound **10d** at CB$_2$R is consistent and can even be detected in a downstream signaling assay.

Figure 5. Pharmacological evaluation of compound **10d**. Each data point and error bar represent the average of 3 independent experiments ± standard error of the mean (SEM). Photoisomers: *cis*-**10d** (purple, dashed line) and *trans*-**10d** (orange, solid line). (A) Radioligand binding assay using *h*CB$_2$R HEK293 membranes. (B) Ligand-induced internalization of FLAG-epitope-tagged *h*CB$_2$R in HEK293 cells.

To confirm βarr-dependency of the experiment for lead compound **10d**, we used arrestin 2/3 siRNA to knockdown βarr-expression and assessed internalization. Consistent with previous findings[44], we have previously shown that CB$_2$R internalization in response to CP55940 requires arrestin proteins, but is independent of Gi/o protein activation.[43a] We verified that this is also the case for internalization of CB$_2$R in response to our lead compound, as significantly less CB$_2$R was internalized upon stimulation with *trans*-**10d** in βarr knockdown cells compared to the control (c.f. **Figure S13**, SI). Thus, for our set of chemically very similar compounds with similar affinities to CB$_2$R, βarr2 bias of compound **10d** was confirmed through preferential selectivity towards the βarr2 endocytic pathway.
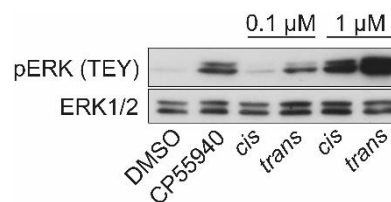
Conclusion

Herein, we report the first βarr2-biased CB$_2$R photoswitchable agonist. By using a non-classical azologization approach with a selective, unbiased CB$_2$R ligand containing the "privileged structure" of benzimidazole, we developed and photocharacterized a novel photoswitchable scaffold of 2-benzimidazole azo-arenes and applied this structure in various pharmacological assays. Modifications of the substitution at the benzene ring were found to have a huge impact on the performance of this class of photoswitch, most noticeable in the varying but sufficiently long thermal half-lives while enabling visible-light photoswitching and resistance to photofatigue. We anticipate the further use of our benzimidazole azo-arenes for the design of tool compounds to obtain spatiotemporal control over distinct biological targets.[27]

Photoswitchable derivatives of **1** selectively bind to CB$_2$R and differences between the respective photoisomers were validated in different biological assays: the benzimidazole azo-arene **10d** was found to be a "*cis*-on" affinity switch at CB$_2$R (radioligand binding) but behaved as a sub-micromolar "*trans*-on" partial agonist efficacy switch in CB$_2$R endocytosis (confocal microscopy and flow cytometry). Ligand **10d** did not show any effect in G protein activation (PLC/CB$_2$R mediated Ca^{2+}-release (concentrations up to 30 µM) and CB$_2$R mini-Gi (concentrations up to 1 µM)). βarr2 bias and dependency were implied in a NanoBit® principle βarr2 recruitment assay and confirmed by looking at CB$_2$R-βarr2 mediated internalization. Downstream

7

RESEARCH ARTICLE

signaling (ERK1/2 activation) further attested to the "*trans*-on"-efficacy behavior of compound **10d**. Thus, ligand **10d** - or future other ligands based on this compound - may find applications in studying the effects of specific activation of the βarr2 pathway at CB_2R and thereby contribute towards elucidating correlations between this specific pathway and the corresponding therapeutically beneficial or adverse effects.

Conflict of Interest

The authors declare no conflict of interest.

Data Availability Statement

The data that support the findings of this study are available in the Supporting Information of this article.

[1] H. C. Lu, K. Mackie, *Biol. Psychiatry* **2016**, *79*, 516-525.

[2] a) A. C. Howlett, M. E. Abood, *Adv. Pharmacol.* **2017**, *80*, 169-206; b) M. Maccarrone, I. Bab, T. Biro, G. A. Cabral, S. K. Dey, V. Di Marzo, J. C. Konje, G. Kunos, R. Mechoulam, P. Pacher, K. A. Sharkey, A. Zimmer, *Trends Pharmacol. Sci.* **2015**, *36*, 277-296; c) S. Galiegue, S. Mary, J. Marchand, D. Dussossoy, D. Carriere, P. Carayon, M. Bouaboula, D. Shire, G. Le Fur, P. Casellas, *Eur. J. Biochem.* **1995**, *232*, 54-61.

[3] a) C. Benito, E. Nunez, R. M. Tolon, E. J. Carrier, A. Rabano, C. J. Hillard, J. Romero, *J. Neurosci.* **2003**, *23*, 11136-11141; b) B. G. Ramirez, C. Blazquez, T. Gomez del Pulgar, M. Guzman, M. L. de Ceballos, *J. Neurosci.* **2005**, *25*, 1904-1913; c) G. A. Cabral, L. Griffin-Thomas, *Expert Rev. Mol. Med.* **2009**, *11*, e3.

[4] J. Ehrhart, D. Obregon, T. Mori, H. Hou, N. Sun, Y. Bai, T. Klein, F. Fernandez, J. Tan, R. D. Shytle, *J. Neuroinflammation* **2005**, *2*, 29.

[5] A. M. Martin-Moreno, D. Reigada, B. G. Ramirez, R. Mechoulam, N. Innamorato, A. Cuadrado, M. L. de Ceballos, *Mol. Pharmacol.* **2011**, *79*, 964-973.

[6] a) D. A. Kendall, G. A. Yudowski, *Front. Cell. Neurosci.* **2016**, *10*, 294; b) G. Navarro, P. Morales, C. Rodriguez-Cueto, J. Fernandez-Ruiz, N. Jagerovic, R. Franco, *Front. Neurosci.* **2016**, *10*, 406; c) E. Aso, I. Ferrer, *Front. Pharmacol.* **2014**, *5*, 37.

[7] A. S. Hauser, M. M. Attwood, M. Rask-Andersen, H. B. Schioth, D. E. Gloriam, *Nat. Rev. Drug Discov.* **2017**, *16*, 829-842.

[8] a) A. Stasiulewicz, K. Znajdek, M. Grudzien, T. Pawinski, A. J. I. Sulkowska, *Int. J. Mol. Sci.* **2020**, *21*, 2778; b) N. Battista, M. Di Tommaso, M. Bari, M. Maccarrone, *Front. Behav. Neurosci.* **2012**, *6*, 9; c) A. Ligresti, S. Petrosino, V. Di Marzo, *Curr. Opin. Chem. Biol.* **2009**, *13*, 321-331.

[9] A. H. Sam, V. Salem, M. A. Ghatei, *J. Obes.* **2011**, *2011*, e432607.

[10] A. Ameri, *Prog. Neurobiol.* **1999**, *58*, 315-348.

[11] a) M. S. Ibsen, M. Connor, M. Glass, *Cannabis Cannabinoid Res.* **2017**, *2*, 48-60; b) T. Kenakin, A. Christopoulos, *Nat. Rev. Drug Discov.* **2013**, *12*, 205-216; c) P. Kolb, T. Kenakin, S. P. H. Alexander, M. Bermudez, L. M. Bohn, C. S. Breinholt, M. Bouvier, S. J. Hill, E. Kostenis, K. A. Martemyanov, R. R. Neubig, H. O. Onaran, S. Rajagopal, B. L. Roth, J. Selent, A. K. Shukla, M. E. Sommer, D. E. Gloriam, *Br. J. Pharmacol.* **2022**, *179*, 3651-3674.

[12] a) A. Dhopeshwarkar, K. Mackie, *J. Pharmacol. Exp. Ther.* **2016**, *358*, 342-351; b) M. Soethoudt, U. Grether, J. Fingerle, T. W. Grim, F. Fezza, L. de Petrocellis, C. Ullmer, B. Rothenhausler, C. Perret, N. van Gils, D. Finlay, C. MacDonald, A. Chicca, M. D. Gens, J. Stuart, H. de Vries, N. Mastrangelo, L. Xia, G. Alachouzos, M. P. Baggelaar, A. Martella, E. D. Mock, H. Deng, L. H. Heitman, M. Connor, V. Di Marzo, J. Gertsch, A. H. Lichtman, M. Maccarrone, P. Pacher, M. Glass, M. van der Stelt, *Nat. Commun.* **2017**, *8*, 13958.

[13] a) T. Ostenfeld, J. Price, M. Albanese, J. Bullman, F. Guillard, I. Meyer, R. Leeson, C. Costantin, L. Ziviani, P. F. Nocini, S. Milleri, *Clin. J. Pain* **2011**, *27*, 668-676; b) P. Morales, P. Goya, N. Jagerovic, *Biochem. Pharmacol.* **2018**, *157*, 8-17.

[14] E. Wouters, J. Walraed, S. D. Banister, C. P. Stove, *Biochem. Pharmacol.* **2019**, *169*, 113623.

[15] J. Mlost, M. Kostrzewa, M. Borczyk, M. Bryk, J. Chwastek, M. Korostynski, K. Starowicz, *Biomed. Pharmacother.* **2021**, *136*, 111283.

[16] a) M. M. Lerch, M. J. Hansen, G. M. van Dam, W. Szymanski, B. L. Feringa, *Angew. Chem. Int. Ed. Engl.* **2016**, *55*, 10978-10999; b) M. J. Fuchter, *J. Med. Chem.* **2020**, *63*, 11436-11447.

[17] D. Lachmann, C. Studte, B. Mannel, H. Hübner, P. Gmeiner, B. König, *Chemistry* **2017**, *23*, 13423-13434.

[18] a) J. Morstein, G. Romano, B. E. Hetzler, A. Plante, C. Haake, J. Levitz, D. Trauner, *Angew. Chem. Int. Ed. Engl.* **2022**, e202117094; b) K. Rustler, G. Maleeva, P. Bregestovski, B. Konig, *Beilstein J. Org. Chem.* **2019**, *15*, 780-788; c) H. Gerwe, F. He, E. Pottie, C. Stove, M. Decker, *Angew. Chem. Int. Ed. Engl.* **2022**, e202203034.

[19] D. Prischich, A. M. J. Gomila, S. Milla-Navarro, G. Sanguesa, R. Diez-Alarcia, B. Preda, C. Matera, M. Batlle, L. Ramirez, E. Giralt, J. Hernando, E. Guasch, J. J. Meana, P. de la Villa, P. Gorostiza, *Angew. Chem. Int. Ed. Engl.* **2021**, *60*, 3625-3631.

[20] L. Agnetta, M. Kauk, M. C. A. Canizal, R. Messerer, U. Holzgrabe, C. Hoffmann, M. Decker, *Angew. Chem. Int. Ed. Engl.* **2017**, *56*, 7282-7287.

[21] a) D. Dolles, A. Strasser, H.-J. Wittmann, O. Marinelli, M. Nabissi, R. G. Pertwee, M. Decker, *Adv. Ther.* **2018**, *1*, 1700032; b) R. C. Sarott, A. E. G. Viray, P. Pfaff, A. Sadybekov, G. Rajic, V. Katritch, E. M. Carreira, J. A. Frank, *J. Am. Chem. Soc.* **2021**, *143*, 736-743; c) T. Hu, G. Zheng, D. Xue, S. Zhao, F. Li, F. Zhou, F. Zhao, L. Xie, C. Tian, T. Hua, S. Zhao, Y. Xu, G. Zhong, Z. J. Liu, A. Makriyannis, R. C. Stevens, H. Tao, *J. Med. Chem.* **2021**, *64*, 13752-13765; d) D. A. Rodriguez-Soacha, J. Fender, Y. A. Ramirez, J. A. Collado, E. Munoz, R. Maitra, C. Sotriffer, K. Lorenz, M. Decker, *ACS Chem. Neurosci.* **2021**, *12*, 1632-1647.

[22] a) S. Pittolo, X. Gomez-Santacana, K. Eckelt, X. Rovira, J. Dalton, C. Goudet, J. P. Pin, A. Llobet, J. Giraldo, A. Llebaria, P. Gorostiza, *Nat. Chem. Biol.* **2014**, *10*, 813-815; b) J. Broichhagen, T. Podewin, H. Meyer-Berg, Y. von Ohlen, N. R. Johnston, B. J. Jones, S. R. Bloom, G. A. Rutter, A. Hoffmann-Roder, D. J. Hodson, D. Trauner, *Angew. Chem. Int. Ed. Engl.* **2015**, *54*, 15565-15569; c) P. Donthamsetti, D. B. Konrad, B. Hetzler, Z. Fu, D. Trauner, E. Y. Isacoff, *J. Am. Chem. Soc.* **2021**, *143*, 8951-8956.

[23] a) V. Sukalovic, D. Andric, G. Roglic, S. Kostic-Rajacic, A. Schrattenholz, V. Soskic, *Eur. J. Med. Chem.* **2005**, *40*, 481-493; b) T. de la Fuente, M. Martin-Fontecha, J. Sallander, B. Benhamu, M. Campillo, R. A. Medina, L. P. Pellissier, S. Claeysen, A. Dumuis, L. Pardo, M. L. Lopez-Rodriguez, *J. Med. Chem.* **2010**, *53*, 1357-1369; c) D. Page, E. Balaux, L. Boisvert, Z. Liu, C. Milburn, M. Tremblay, Z. Wei, S. Woo, X. Luo, Y. X. Cheng, H. Yang, S. Srivastava, F. Zhou, W. Brown, M. Tomaszewski, C. Walpole, L. Hodzic, S. St-Onge, C. Godbout, D. Salois, K. Payza, *Bioorg. Med. Chem. Lett.* **2008**, *18*, 3695-3700.

[24] a) D. Dolles, M. Nimczick, M. Scheiner, J. Ramler, P. Stadtmuller, E. Sawatzky, A. Drakopoulos, C. Sotriffer, H. J. Wittmann, A. Strasser, M. Decker, *ChemMedChem* **2016**, *11*, 1270-1283; b) D. M. Carter, E. Specker, P. H. Malecki, J. Przygodda, K. Dudaniec, M. S. Weiss, U. Heinemann, M. Nazare, U. Gohlke, *J. Med. Chem.* **2021**, *64*, 14266-14282.

[25] M. P. Windisch, S. Jo, H. Y. Kim, S. H. Kim, K. Kim, S. Kong, H. Jeong, S. Ahn, Z. No, J. Y. Hwang, *Eur. J. Med. Chem.* **2014**, *78*, 35-42.

[26] K. Wu, X. Peng, M. Chen, Y. Li, G. Tang, J. Peng, Y. Peng, X. Cao, *Chem. Biol. Drug Des.* **2022**, *99*, 736-757.

[27] a) S. Tahlan, S. Kumar, B. Narasimhan, *BMC Chem.* **2019**, *13*, 101; b) G. Yadav, S. Ganguly, *Eur. J. Med. Chem.* **2015**, *97*, 419-443.

[28] M. Gaba, C. Mohan, *Med. Chem. Res.* **2015**, *25*, 173-210.

[29] D. Page, M. C. Brochu, H. Yang, W. Brown, S. St-Onge, E. Martin, D. Salois, *Lett. Drug. Des. Discov.* **2006**, *3*, 298-303.

[30] S. Crespi, N. A. Simeth, B. König, *Nat. Rev. Chem.* **2019**, *3*, 133-146.

[31] a) S. N. Kolodyazhnaya, A. M. Simonov, *Chem. Heterocycl. Compd.* **1967**, *3*, 304-304; b) A. M. Simonov, S. N. Kolodyazhnaya, *Chem. Heterocycl. Compd.* **1970**, *6*, 1459-1462; c) R. A. Sogomonova, A. M. Simonov, L. N. Divaeva, S. N. Kolodyazhnaya, *Chem. Heterocycl. Compd.* **1982**, *18*, 620-626; d) M. N. Matada, K. Jathi, P. Malingappa, I. Pushpavathi, *Chem. Data Collect.* **2020**, *25*, 100314; e) D. Sarkar, A. K. Pramanik, T. K. Mondal, *Spectrochim. Acta. A Mol. Biomol. Spectrosc.* **2016**, *153*, 397-401; f) S. E. Korolenko, K. P. Zhuravlev, V. I. Tsaryuk, A. S. Kubasov, V. V. Avdeeva, E. A. Malinina, A. S. Burlov, L. N. Divaeva, K. Y. Zhizhin, N. T. Kuznetsov, *J. Lumin.* **2021**, *237*, 118156; g) H. Hessoon, F. Karam *Egypt. J. Chem.* **2021**, *65*, 327-334; h) S. Okumura, C. H. Lin, Y. Takeda, S. Minakata, *J. Org. Chem.* **2013**, *78*, 12090-12105.

[32] M. Scheiner, D. Dolles, S. Gunesch, M. Hoffmann, M. Nabissi, O. Marinelli, M. Naldi, M. Bartolini, S. Petralla, E. Poeta, B. Monti, C. Falkeis, M. Vieth, H. Hubner, P. Gmeiner, R. Maitra, T. Maurice, M. Decker, *J. Med. Chem.* **2019**, *62*, 9078-9102.

[33] J. Calbo, C. E. Weston, A. J. White, H. S. Rzepa, J. Contreras-Garcia, M. J. Fuchter, *J. Am. Chem. Soc.* **2017**, *139*, 1261-1274.

[34] J. Broichhagen, J. A. Frank, D. Trauner, *Acc. Chem. Res.* **2015**, *48*, 1947-1960.

[35] J. Otsuki, K. Suwa, K. K. Sarker, C. Sinha, *J. Phys. Chem. A* **2007**, *111*, 1403-1409.

[36] J. Garcia-Amoros, D. Velasco, *Beilstein J. Org. Chem.* **2012**, *8*, 1003-1017.

[37] A. D. W. Kennedy, I. Sandler, J. Andreasson, J. Ho, J. E. Beves, *Chemistry* **2020**, *26*, 1103-1110.

[38] R. Lin, P. K. Hashim, S. Sahu, A. S. Amrutha, N. M. Cheruthu, S. Thazhathethil, K. Takahashi, T. Nakamura, T. Kikukawa, N. Tamaoki, *J. Am. Chem. Soc.* **2023**, *145*, 9072–9080 .

[39] W. A. Velema, W. Szymanski, B. L. Feringa, *J. Am. Chem. Soc.* **2014**, *136*, 2178-2191.

[40] A. S. Dixon, M. K. Schwinn, M. P. Hall, K. Zimmerman, P. Otto, T. H. Lubben, B. L. Butler, B. F. Binkowski, T. Machleidt, T. A. Kirkland, M. G. Wood, C. T. Eggers, L. P. Encell, K. V. Wood, *ACS Chem. Biol.* **2016**, *11*, 400-408.

[41] X. Chen, C. Zheng, J. Qian, S. W. Sutton, Z. Wang, J. Lv, C. Liu, N. Zhou, *Curr. Mol. Pharmacol.* **2014**, *7*, 67-80.

[42] M. Grundmann, N. Merten, D. Malfacini, A. Inoue, P. Preis, K. Simon, N. Ruttiger, N. Ziegler, T. Benkel, N. K. Schmitt, S. Ishida, I. Muller, R. Reher, K. Kawakami, A. Inoue, U. Rick, T. Kuhl, D. Imhof, J. Aoki, G. M. Konig, C. Hoffmann, J. Gomeza, J. Wess, E. Kostenis, *Nat. Commun.* **2018**, *9*, 341.

[43] a) A. Tutov, S. A. M. Steinmüller, Y. A. Ramírez, C. E. Jack, D. A. R. Soacha, C. A. Sotriffer, J. N. Hislop, M. Decker, *Adv. Ther.* **2023**, *6*, 2200260; b) D. Thompson, S. McArthur, J. N. Hislop, R. J. Flower, M. Perretti, *J. Biol. Chem.* **2014**, *289*, 36166-36178.

[44] B. K. Atwood, J. Wager-Miller, C. Haskins, A. Straiker, K. Mackie, *Mol. Pharmacol.* **2012**, *81*, 250-263.

[45] a) A. Tomasovic, T. Brand, C. Schanbacher, S. Kramer, M. W. Hummert, P. Godoy, W. Schmidt-Heck, P. Nordbeck, J. Ludwig, S. Homann, A. Wiegering, T. Shaykhutdinov, C. Kratz, R. Knuchel, H. K. Muller-Hermelink, A. Rosenwald, N. Frey, J. Eichler, D. Dobrev, A. El-Armouche, J. G. Hengstler, O. J. Muller, K. Hinrichs, F. Cuello, A. Zernecke, K. Lorenz, *Nat. Commun.* **2020**, *11*, 1733; b) D. A. Rodriguez-Soacha, S. A. M. Steinmüller, A. Isbilir, J. Fender, M. H. Deventer, Y. A. Ramirez, A. Tutov, C. Sotriffer, C. P. Stove, K. Lorenz, M. J. Lohse, J. N. Hislop, M. Decker, *ACS Chem. Neurosci.* **2022**, *13*, 2410-2435.

9

RESEARCH ARTICLE

Entry for the Table of Contents
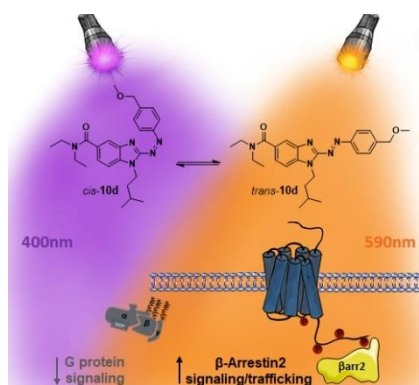
A new photoswitchable scaffold was developed based on the "privileged structure" of benzimidazole: 2-benzimidazole azo-arenes. This scaffold was used for the development of functionally selective CB$_2$R ligands with βarr2 bias. Compound **10d** acts as a "*trans*-on"-efficacy switch in βarr2-mediated endocytosis and can be used to investigate the CB$_2$R-βarr2 endocytic pathway.